Acta Geochim (2021) 40(4):525–531
https://doi.org/10.1007/s11631-021-00473-3

ORIGINAL ARTICLE

Pressure calibration and sound velocity measurement to 12 GPa in multi-anvil apparatus

Wei Song[1] · Shuangming Shan[1] · Qizhe Tang[2] · Chang Su[3] · Yonggang Liu[1]

Received: 26 January 2021 / Revised: 4 March 2021 / Accepted: 29 March 2021 / Published online: 13 April 2021

Abstract We performed the pressure calibration to 12 GPa for 14/6 type (octahedron edge length/WC truncated edge length, in mm) cell assembly in DS 6 × 1400 multi-anvil apparatus by using the phase transitions in Bi (I-II 2.55 GPa, III-V 7.67 GPa) and ZnTe (LPP-HPP I 9.6 GPa, HPP I-II 12.0 GPa). As verification and application, sound velocity measurements on polycrystalline Al_2O_3 to 12 GPa at room temperature were conducted and the ultrasonic result is in good agreement with previous reports. It demonstrates the feasibility of performing sound velocity measurements close to the mantle transition zone pressure condition in our laboratory.

Keywords Pressure calibration · Sound velocity · Multi-anvil apparatus · Polycrystalline alumina

1 Introduction

Simulating the high-pressure and high-temperature conditions of the Earth's interiors is crucial for the studies of Earth and planets since most of their mass is located at depths that are inaccessible to direct investigation. In general, the static high-pressure apparatus used to simulate can be divided into diamond anvil cell (DAC) and large volume press (LVP), multi-anvil apparatus (MAA) is the representative of the latter. Sound velocity measurements of millimeter-sized polycrystalline specimens in MAA play an important role in high-pressure science and geoscience because it can provide accurate measurements of compressional (P) and shear (S) wave velocity and hence the elasticity of rocks and minerals of geological importance and other materials.

Since sound velocities of minerals and rocks under high temperature and pressure are extremely important physical parameters for understanding the composition, structure, and thermodynamic properties of the Earth's interior (Li et al. 1998; Ritsema et al. 2004; Gréaux et al. 2019; Marquardt and Thomson 2020). The deeper in the Earth's interiors means the higher pressure. Many scientists attempted to extend the experimental pressure and get more accurate results for sound velocity measurements in MAA (Kinoshita et al. 1979; Fujisawa and Ito 1984, 1985; Kosuki et al. 1986; Yoneda 1990; Song et al. 2005). Baosheng Li and coworkers at Stony Brook University (USA) made an outstanding contribution to the progress of sound velocity measurements in MAA. Li et al. (1996) developed a new method for velocity measurement in MAA and applied it to dense fine-grained polycrystalline alumina velocity experiments at 10 GPa, which feature a stress-free transducer location and sample-friendly cell assemblies. Later, the X-ray diffraction (Liebermann et al. 1998; Li et al. 2001, 2004) and X-radiography technique (Kung et al. 2002, 2004) were also utilized in MAA, allowing for simultaneous measurements of compressional and shear wave travel times, cell pressure, density and sample length under high-pressure experiments (Li et al. 2005; Li and Liebermann 2014). Since then, state-of-the-art techniques for sound velocity measurements in MAA were built and lots of subsequent velocity experiments in

✉ Yonggang Liu
liuyonggang@vip.gyig.ac.cn

[1] Key Laboratory of High-Temperature and High-Pressure Study of the Earth's Interior, Institute of Geochemistry, Chinese Academy of Sciences, Guiyang 550081, China

[2] School of Information Engineering, Huzhou University, Huzhou 313000, China

[3] Institute of Disaster Prevention, Sanhe 065201, China

MAA were affected or benefitted by those techniques. At present, sound velocity measurements in MAA have already reached 27 GPa (Higo et al. 2018) and 2375 K (Xu et al. 2018), corresponding to the lower mantle P–T conditions, respectively. The current highest pressure and temperature of sound measurement in MAA and DAC are shown in Fig. 1. More details of experimental techniques of sound measurement under deep mantle conditions are given by Marquardt and Thomson (2020).

In China, Prof. Hongsen Xie and his coworkers in the Institute of Geochemistry, Chinese Academy of Sciences pioneered the ultrasonic measurements in MAA and made great achievements (Xie et al. 1993, 1998, 2002). However, no matter solid sample (Liu et al. 2000, 2002; Zhou et al. 2011; He et al. 2014; Xu et al. 2014) or liquid sample experiments (Song et al. 2011; Wang et al. 2013; Su et al. 2017), the sound velocity measurements in MAA in China are still usually limited to relatively low pressure (below 5.5 GPa), beyond the reach of the focused area in the mantle, for example, the transition zone (410 $\sim$ 660 km, 14–24 GPa), and the lacking higher pressure apparatus may account for this dilemma. Note that, when limited by the intrinsic properties of the first stage tungsten carbide (WC) anvil in MAA, the attainable pressure using the first stage anvil is normally several GPa. Consequently, the second stage anvil system is applied in MAA for the generation of higher pressure. In the last decade, more and more research institutes started to install MAA for scientific or industrial applications in China. Recently, Zhou et al. (2016) set up a new ultrasonic velocity measurements system in an MAA installed in China University of Geosciences (Wuhan) and measured the velocities of polycrystalline wadsleyite to 18 GPa. Ren and Li (2018) calibrated the pressure for 10/4 type cell assembly to 19 GPa in DS 6 $\times$ 1400 t multi-anvil apparatus installed in Institute of Geochemistry by using

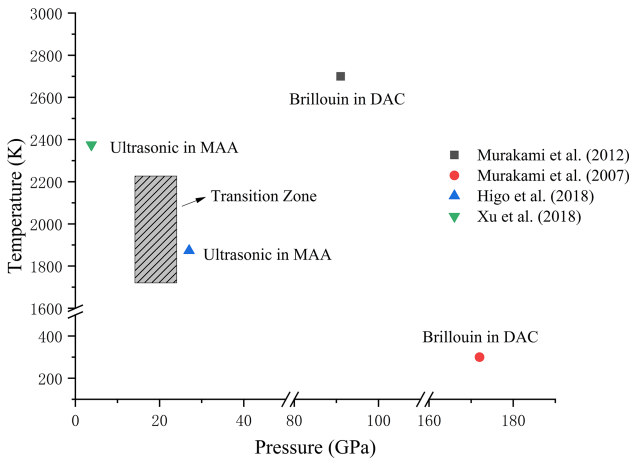

Fig. 1 Current highest pressure and temperature of sound velocity measurement in MAA and DAC

the transitions in ZnTe, ZnS, and GaAs, but no sound velocity experiment was conducted.

Also, methods for pressure determination in high-pressure apparatus generally include the so-called fixed-point calibration and continuous calibration, the former is based on phase transitions of metals and semiconductors (e.g. Bi, Ba, ZnTe, ZnS, and GaAs) and the latter is to build relationships between pressure and certain experimentally measurable properties of a calibrant, such as changes in resistance (e.g. manganin), unit-cell volume (e.g. NaCl, Au), peak shifts in fluorescence (Ruby) and Raman spectra (diamond, c-BN). It's worth mentioning that travel times in calibrants also can be used for pressure calibration (Wang et al. 2015; Song et al. 2020).

In this paper, we presented the results of pressure calibration for 14/6 type cell assembly to 12 GPa in DS 6 $\times$ 1400 t multi-anvil apparatus installed in our laboratory by using the phase transitions in Bi and ZnTe, then applied it to the sound velocity measurements on polycrystalline Al_2O_3 to 12 GPa at room temperature.

2 Experimental method

The experiments were performed in a 6–8 cubic-type MAA (DS6 $\times$ 1400t), which is capable of generating oil pressures up to 40 MPa, at the Key Laboratory for High-Temperature and High-Pressure Study of the Earth's Interior, Institute of Geochemistry, Chinese Academy of Sciences, China. The press consists of six first-stage anvils made of WC, which enclose a cubic cavity of 44.5 mm edge length. The eight-second stage anvils used in this work are also made of WC, which have a 24 mm edge length and one corner truncated into a triangular surface with a 6 mm edge length. The truncations enclose an octahedral cavity holding the sample assembly. The second stage anvils are separated by pyrophyllite gaskets and insulated from the first stage anvils by epoxy resin sheets. The octahedron of the sample assembly has a 14 mm edge length and is made of MgO to transfer pressure.

In pressure calibration experiments, Bi wire and powdered ZnTe (both 99.99% purity) were used as samples and changes in electrical resistance associated with phase transitions in Bi (I-II 2.55 GPa, III-V 7.67 GPa, Decker et al. 1972) and ZnTe (LPP-HPP I 9.6 GPa, HPP I-II 12.0 GPa, LPP: Low-Pressure Phase; HPP: High-Pressure Phase, Kusaba et al. 1993) served to calibrate the pressure. Figure 2 shows the schematic diagram of sample assemblies for resistance measurements in the DS 6 $\times$ 1400 t apparatus. The pressure calibrant placed in MgO octahedron is connected to a multimeter (Agilent 34410A, USA) to measure resistance continuously by sets of copper wires, and the two diagonally opposite WC second anvils served

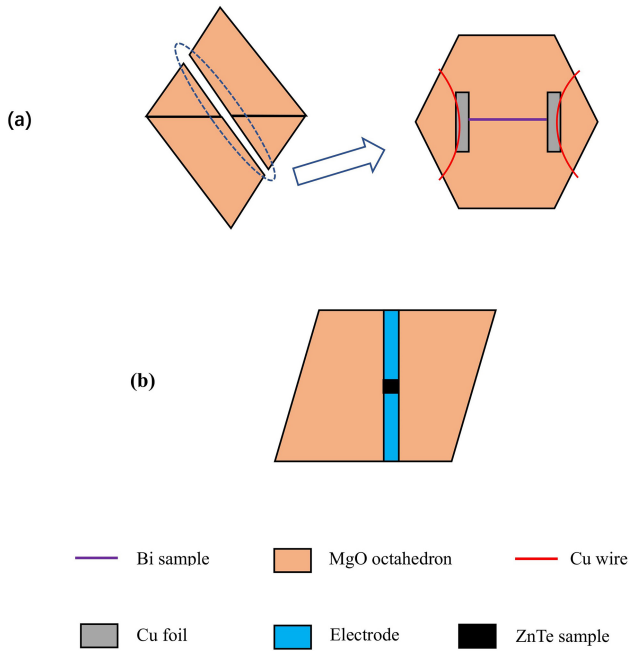

Fig. 2 The schematic diagram of sample assemblies for resistance measurements in DS 6 × 1400 t apparatus: (**a**) is for the resistance measurement of Bi, in which a whole MgO octahedron was cut into two halves along the midpoint of edges (left) in which the Bi calibrant and conducting unit were placed (right); (**b**) is for the resistance measurement of ZnTe

as conducting medium. The resistance was measured by the four-wire method in Bi experiments and the two-wire method in ZnTe experiments, respectively.

Figure 3 shows the schematic diagram of sample assembly for velocity measurements at room temperature used in this work. The transducer was mounted on one truncation of the second anvil and this anvil thus served as the buffer rod to transmit the acoustic signal. The dense polycrystalline Al_2O_3 sample (99.99% purity, 3 mm in length, 2 mm in diameter) was positioned flush with the surface of the octahedron and surrounded by boron nitride (BN, 1 mm wall thickness), thereby providing a pseudo-hydrostatic pressure condition to prevent the sample from cracking at high pressure. A thin copper foil (0.01 mm thickness) was inserted between the WC buffer rod and sample to enhance mechanical coupling. To minimize the acoustic energy loss, all contact interfaces include the buffer rod and sample were well polished before the measurements. Al_2O_3 was chosen as a test sample for the following reasons: (1) commercially available (2) high elastic moduli thus stable under high pressure (3) suitable acoustic impedance (4) known elastic properties in literature satisfies comparison of results.

The ultrasonic travel times were measured with the classical pulse-echo method by using a longitudinal wave 20 MHz $LiNbO_3$ transducer (BPO INC. USA), a digital oscilloscope (Tektronix DPO2024B, USA), and an ultrasonic pulse generator/receiver unit (Panametrics 5077PR, USA). A typical longitudinal wave signal observed under high pressure is shown in Fig. 4. In Figs. 3 and 4, Echo 1 and Echo 2 represent the longitudinal wave signal reflected from the buffer rod–sample and the sample–BN interfaces, respectively. The travel time in the sample was determined by the interval between the two corresponding peaks shown in Fig. 4. The travel time measurement sensitivity is 1 ns, the travel time in the sample is about 0.5 μs, and so the relative error of the travel time in the sample is about 0.4%

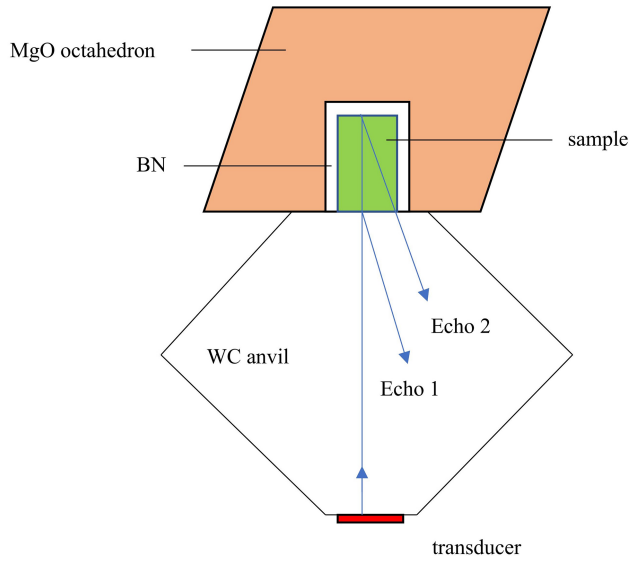

Fig. 3 The schematic diagram of sample assembly for ultrasonic measurements in DS 6 × 1400 t apparatus. Echo 1: WC buffer rod; Echo 2: sample

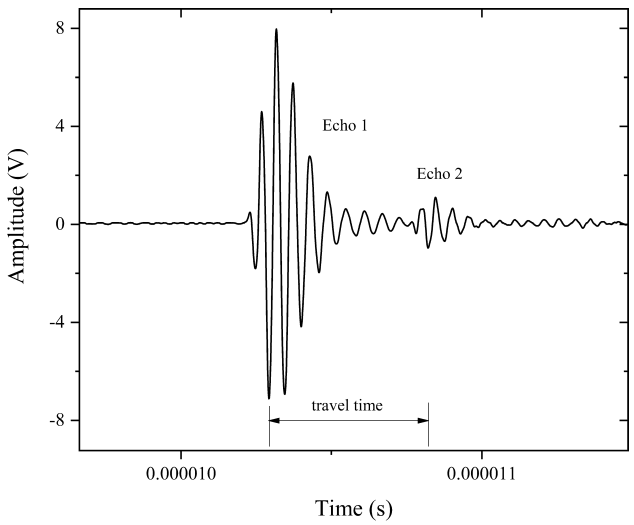

Fig. 4 A typical longitudinal wave signal observed at 4 GPa. Echo 1: WC buffer rod; Echo 2: sample

(considering the two values obtained from the two corresponding signals, respectively).

3 Results and discussion

The results of electrical resistance measurements are shown in Fig. 5 for Bi and Fig. 6 for ZnTe, from which the phase transitions can be easily recognized directly. As can be seen in Fig. 5, it is obvious that around oil pressure 2.48(±0.1) MPa and 8.48(±0.2) MPa, the resistance starts to decrease sharply, corresponding to the phase transitions of Bi I-II and III-V, respectively.

For the criteria of phase transition points, it normally consists of the turning point and the midpoint method, which may have little difference as the process of phase transition is quick enough. Some investigators suggested that the pressure at which the phase transition starts is slightly higher than the thermodynamic equilibrium pressure of phase transition, which is the fixed-point pressure scale of a given pressure calibrant (Xie 1997). In this situation, the midpoint method seems to be more accurate. In this way, we used the midpoint method to determine phase transition points in Fig. 5. But even so, it may have little effect on the pressure calibration.

In Fig. 6, the behavior of resistance change of ZnTe was quite similar to that in the previous studies (Ohtani et al. 1980; Kusaba et al. 1993; Nishiyama et al. 2008), a turning point appears at oil pressure 9.45(±0.3) MPa, at which the electrical resistance started increasing, corresponding to the phase transition of ZnTe LPP-HPP I. The phase transition of ZnTe HPP I-II is determined by the midpoint of a large resistance decrease of four orders of magnitude, that is 15.68(±0.2) MPa oil pressure. Different from the processes of phase transitions of Bi in Fig. 5, the processes of phase

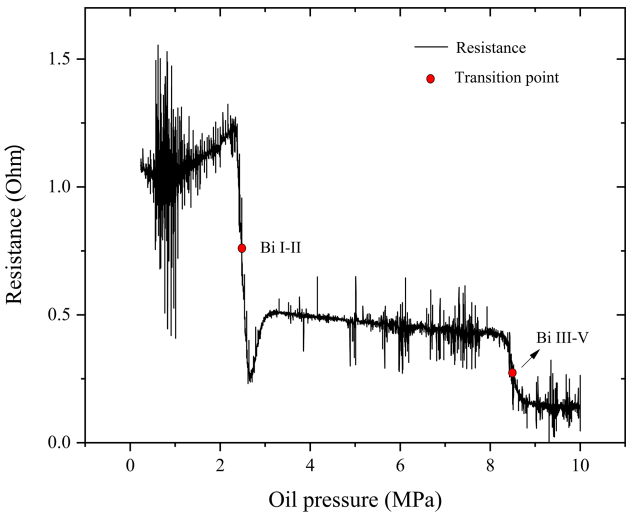

Fig. 5 Resistance change of Bi as a function of oil pressure

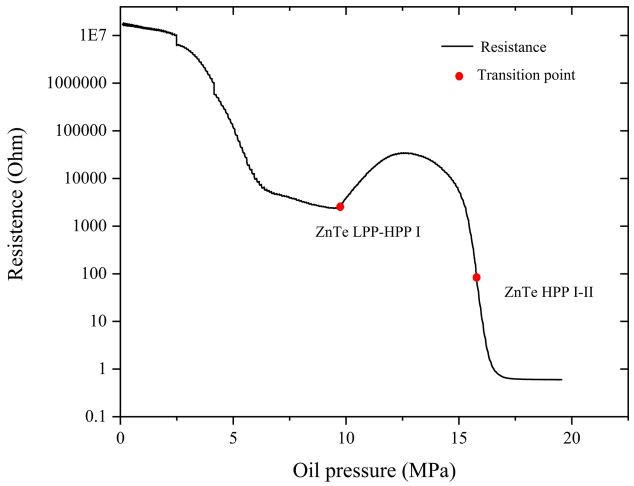

Fig. 6 Resistance change of ZnTe as a function of oil pressure

transitions of ZnTe in Fig. 6 are relatively slower, especially the ZnTe LPP-HPP phase transition, at which the turning point of resistance increasing is quite clear. On the other hand, when focusing on the part where the resistance decreases fastest in the ZnTe HPP I-II transition, the phase transition point becomes clear and accurate. In this way, we routinely used the turning point method in the ZnTe LPP-HPP transition and midpoint method in the ZnTe HPP I-II transition to determine phase transition point, respectively.

In addition, there is another anomaly around 6.4 MPa, at which the trend of reduction in resistance is noticeably slower. But compared with the two other higher-pressure anomalies, which could be explained by volume change at phase transitions in ZnTe, this anomaly was attributed to a change of band gap in the zinc blende type ZnTe and there is no phase transition occurs near this anomaly.

Consequently, with the known phase transition pressure of Bi and ZnTe calibrants, combining the four observed points and the zero-pressure value, the pressure can be calibrated and the result is shown in Fig. 7. After polynomial fitting, the pressure calibration curve is expressed as $P(\mathrm{GPa}) = -0.0293P_{oil}^2 + 1.2374P_{oil} - 0.1456$, where P_{oil} is oil pressure in MPa. According to Decker et al. (1972) and Kusuba et al. (1993), the errors of phase transitions pressure were 0.006 GPa for Bi I-II, 0.18 GPa for Bi III-V, 0.2 GPa for ZnTe LPP-HPP I, and 0.2 GPa for ZnTe HPP I-II, so the maximum pressure error in this study is estimated to about 3%, as the system error is also taken into account.

Note that, when using ZnTe as calibrant for pressure determination, the grain size effect of the starting material should be given attention, since the ZnTe HPP I-II phase transition pressure is 12 GPa for powdered ZnTe and 13 GPa for single crystal ZnTe, respectively. The ZnTe LPP-

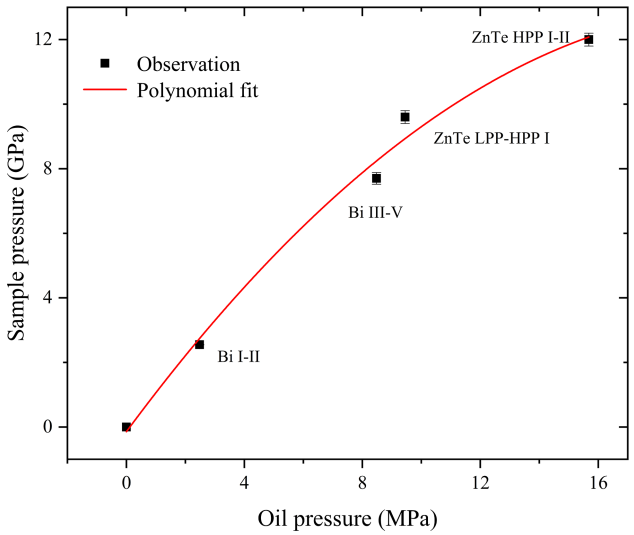

Fig. 7 The relation between sample pressure and oil pressure

HPP phase transition pressure is independent of such a grain size effect (Kusuba et al. 1993).

While ultrasonic experiments can obtain precise measurements of travel times, the length of the sample is needed for the calculation of wave velocities at high pressure. In the case of lacking X-ray sources (X-radiography), the length of the sample at high pressure is dependent on correct computing. Normally, with the measured P and S wave travel times in the sample, the length change of the sample at high pressures can be obtained by an approach known as Cook's method (Cook 1957; Li and Liebermann 2014). Cook's method has been frequently used in high-pressure ultrasonic studies when direct sample length measurements were not available. But in this work, we only installed a longitudinal wave transducer that cannot obtain shear wave travel time. Alternatively, we can use a method that comprises the following empirical equation to correct the elastic shortening of the sample at high pressure (Ito et al. 1977):

$$\frac{l_0}{l} = 1 + \frac{P}{3K_{T0}} \tag{1}$$

where l, l_0 are sample length at high pressure and zero pressure, P is pressure, K_{T0} is zero pressure isothermal bulk moduli. Then we can use the following well-known equations to calculate the sample length:

$$K_{T0} = K_{S0}/(1 + \alpha\gamma T) \tag{2}$$

$$K_{S0} = \rho_0\left(V_{p0}^2 - \frac{4}{3}V_{s0}^2\right) \tag{3}$$

where K_{S0} is adiabatic bulk moduli, α is the thermal expansion coefficient, γ is the Grüeisen parameter, T is absolute temperature, ρ_0 is the density at zero pressure, V_{p0} and V_{s0} are compressional and shear wave velocity at zero pressure, which was measured separately at benchtop with a larger diameter sample. We found that the calculated K_{S0} value in this work is 1.7% less than that of Li et al. (1996), but in close agreement (< 0.2%) with those of Kung et al. (2000) and Higo et al. (2006). Accordingly, the sound velocity of polycrystalline Al_2O_3 sample at high pressure can be calculated (the used relevant parameters are listed in Table 1) and the results are shown in Fig. 8. As compared with previous ultrasonic results in Fig. 8, our measured results are in good agreement with those of Li et al. (1996) and Kung et al. (2000) and slightly higher than those of Higo et al. (2006). After linear fitting, the sound velocity results from this work are expressed as $V_p\ (km/s) = 10.875 + 0.063P\ (GPa)$, $R^2 = 0.99$. The average pressure derivative of V_p from this study is slightly higher than those previous results in Fig. 8, and this is probably the combined effect of error of pressure calibration and deviator stress. The uncertainty of velocity measurement is related to the determination of sample length, travel time, and pressure. According to the above formula referring to V_p, the effect of pressure error (3%) on the V_p is estimated to have a maximum error of 0.2% at the highest pressure. On the other hand, when using empirical Eq. (1) to evaluate sample length at high pressure, the uncertainty of length is estimated to be about 0.2%. Then combining the uncertainty of travel time (0.4%), we believed that the whole uncertainty of sound velocity is about 1%. Therefore, it confirms not only the validation of the pressure calibration in this work but also the ability to perform sound velocity measurements close to the pressure condition of the mantle transition zone in our laboratory.

4 Conclusion

In this work, we performed the pressure calibration to 12 GPa for 14/6 type cell assembly in DS 6 × 1400 multi-anvil apparatus using the phase transitions in Bi (I-II 2.55, III-V 7.67 GPa) and ZnTe (LPP-HPP I 9.6 GPa, HPP I-II 12.0 GPa) at room temperature. A subsequent sound velocity experiment of polycrystalline Al_2O_3 was conducted to test the validation of the results of the pressure calibration. Since the tested result is positive, it makes our lab become one of the few domestic labs which can perform sound velocity measurements in MAA close to the mantle transition zone pressure condition and it should be valuable to later studies of the elastic properties of mantle minerals. However, so far, there is no synchrotron X-ray source in the sound velocity measurements in MAA in China, the pressure calibration work has to be usually performed under ex situ conditions. Pressure calibration under in situ conditions should in principle get more accurate results and this is our object in the future.

Table 1 The zero pressure isothermal bulk moduli (K_{T0}) of polycrystalline Al_2O_3 sample and the used relevant parameters at ambient condition for calculation

$1 + \alpha\gamma T$	ρ_0 (g/cm^3)	V_{p0} (km/s)	V_{s0} (km/s)	K_{S0} (GPa)	K_{T0} (GPa)
1.006437*	3.98	10.87	6.40	252.9	251.3

*Schrerber and Anderson (1966)

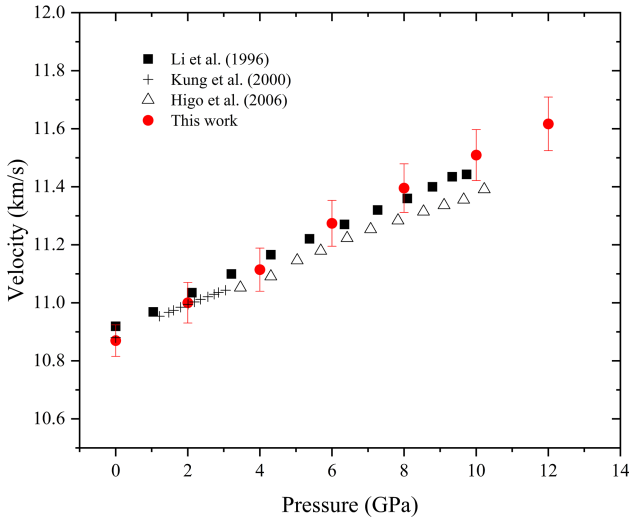

Fig. 8 Comparison of sound velocity of polycrystalline Al_2O_3 under high pressure

Meanwhile, temperature, higher pressure, and V_s measurement also needs to be placed on the agenda for the improvement of experimental techniques.

Acknowledgements This work was supported by the National Natural Science Foundation of China under Grant No. 41873075 and the West Light Foundation of The Chinese Academy of Sciences.

Declarations

Conflict of interest The authors declare that they have no conflict of interest.

References

Cook RK (1957) Variation of elastic constants and static strains with hydrostatic pressure: a method for calculation from ultrasonic measurements. J Acous Soc Am 29:445–449

Decker DL, Bassett WA, Merrill L, Hall HT, Barnett JD (1972) High-pressure calibration: a critical review. J Phys Chem Ref Data 1:773–836

Fujisawa H, Ito E (1984) Measurement of ultrasonic wave velocities in solid under high pressure. Jpn J Appl Phys 23:51–53

Fujisawa H, Ito E (1985) Measurement of ultrasonic wave velocities of tungsten carbide as a standard material under high pressures up to 8 GPa. Jpn J Appl Phys 24:103–105

Gréaux S, Irifune T, Higo Y, Tange Y, Arimoto T, Liu ZD, Yamada A (2019) Sound velocity of $CaSiO_3$ perovskite suggests the presence of basaltic crust in the Earth's lower mantle. Nature 565:218–221

He Z, Wang ZG, Zhu HY, Liu XR, Peng JP, Hong SM (2014) High-pressure behavior of amorphous selenium from ultrasonic measurements and Raman spectroscopy. Appl Phys Lett 105:011901

Higo Y, Inoue T, Li BS, Irifune T, Liebermann RC (2006) The effect of iron on the elastic properties of ringwoodite at high pressure. Phys Earth Planet Inter 159:276–285

Higo Y, Irifune T, Funakoshi K (2018) Simultaneous high-pressure high-temperature elastic velocity measurement system up to 27 GPa and 1873 K using ultrasonic and synchrotron X-ray techniques. Rev Sci Instrum 89:014501

Ito H, Mizutani H, Ichinose K, Akimoto S (1977) Ultrasonic wave velocity measurements in solids under high pressure using solid pressure media. In: Manghnani MH, Akimoto SI (eds) High pressure research: applications in geophysics. Academic press, New York, pp 603–622

Kinoshita H, Hamaya N, Fujisawa H (1979) Elastic properties of single-crystal NaCl under high pressures to 80 kbar. J Phys Earth 27:337–350

Kosuki Y, Yoneda A, Fujimura A, Sawamoto H, Kumazawa M (1986) Generation of large volume hydrostatic pressure to 8 GPa for ultrasonic studies. Jpn J Appl Phys 25:1427–1430

Kung J, Rigden S, Gwanmesia G (2000) Elasticity of $ScAlO_3$ at high pressure. Phys Earth Planet Inter 118:65–75

Kung J, Li BS, Weidner J, Zhang JZ, Liebermann RC (2002) Elasticity of $(Mg_{0.83}, Fe_{0.17})O$ ferropericlase at high pressure: ultrasonic measurements in conjunction with X-radiation techniques. Phys Earth Planet Inter 203:557–566

Kung J, Li BS, Uchida T, Wang YB, Neuville D, Liebermann RC (2004) In situ measurements of sound velocities and densities across the orthopyroxene → high-pressure clinopyroxene transition in $MgSiO_3$ at high pressure. Phys Earth Planet Inter 147:27–44

Kusaba K, Galoisy L, Wang YB, Vaughan MT, Weidner DJ (1993) Determination of phase transition pressure of ZnTe under quasihydrostatic conditions. PAGEOPH 141:040643–040652

Li BS, Kung J (2005) Pressure calibration to 20 GPa by simultaneous use of ultrasonic and X-ray techniques. J Appl Phys 98:013521

Li BS, Liebermann RC (2014) Study of the Earth's interior using measurements of velocities in minerals by ultrasonic interferometry. Phys Earth Planet Inter 223:135–153

Li BS, Jackson I, Gasparik T, Liebermann RC (1996) Elastic wave velocity measurement in multi-anvil apparatus to 10 GPa using ultrasonic interferometry. Phys Earth Planet Inter 98:79–91

Li BS, Liebermann RC, Weidner DJ (1998) Elastic Moduli of Wadsleyite (β-Mg_2SiO_4) to 7 Gigapascals and 873 Kelvin. Science 281:675–676

Li BS, Liebermann RC, Weidner DJ (2001) P-V-Vp-Vs-T measurements on wadsleyite to 7 GPa and 873 K: implications for the 410-km seismic discontinuity. J Geophys Res 106:30575–30591

Li BS, Kung J, Liebermann RC (2004) Modern techniques in measuring elasticity of earth materials at high pressure and high temperature using ultrasonic interferometry in conjunction with

synchrotron X-radiation in multi-anvil apparatus. Phys Earth Planet Inter 143–144:559–574

Liebermann RC, Chen G, Li B, Gwanmesia GD, Chen J, Vaughan MT, Weidner DJ (1998) Sound velocity measurements in oxides and silicates at simultaneous high pressures and temperatures using ultrasonic techniques in multi-anvil apparatus in conjunction with synchrotron X-radiation determination of equation of state. Rev High Pressure Sci Technol 7:75–78

Liu YG, Xie HS, Guo J, Zhou WG, Xu JA, Zhao ZD (2000) A new method for experimental determination of compressional velocities in rocks and minerals at high-pressure. Chin Phys Lett 17:924–926

Liu YG, Xie HS, Zhou WG, Guo J (2002) A method for experimental determination of compressional velocities in rocks and minerals at high pressure and high temperature. J Phys Condens Matter 14:11381–11384

Marquardt H, Thomson AR (2020) Experimental elasticity of Earth's deep mantle. Nat Rev Earth Environ 1:455–469

Murakami M, Sinogeikin SV, Bass JD, Sata N, Ohishi Y, Hirose K (2007) Sound velocity of $MgSiO_3$ post-perovskite phase: A constraint on the D″ discontinuity. Earth Planet Sci Lett 259:18–23

Murakami M, Ohishi Y, Hirao N, Hirose K (2012) A perovskitic lower mantle inferred from high-pressure, high-temperature sound velocity data. Nature 485:90–94

Nishiyama N, Wang YB, Sanehira T, Irifune T, Rivers ML (2008) Development of the multi-anvil assembly 6–6 for DIA and D-DIA type high-pressure apparatuses. High Pressure Res 28:307–314

Ohtani A, Motobayashi M, Onodera A (1980) Polymorphism of ZnTe at elevated pressure. Phys Lett 75A:435–437

Ren DS, Li HP (2018) Pressure calibration for two-stage 6–8 type large-volue multi-anvil high pressure apparatus. Acta Mineralogica Sinica 38:355–358 **(in Chinese)**

Ritsema J, van Heijst HJ, Woodhous JH (2004) Global transition zone tomography. J Geophys Res Solid Earth 109:B02302

Schrerber E, Anderson O (1966) Pressure derivatives of the sound velocities of polycrystalline alumina. J Am Ceram Soc 49:184–190

Song MS, Yoneda A, Ito E (2005) Solid–liquid hybrid assembly for ultrasonic elasticity measurements under hydrostatic conditions of up to 8GPa in a Kawai-type multianvil apparatus. Rev Sci Instrum 76:033906

Song W, Liu YG, Wang ZG, Gong CY, Guo J, Zhou WG, Xie HS (2011) Note: measurement method for sound velocity of melts in large volume press and its application to liquid sodium up to 2.0 GPa. Rev Sci Instru 82:086108

Song W, Tang QZ, Su C, Chen X, Liu YG (2020) Pressure calibration based on the ultrasonic measurement in multi-anvil apparatus. High Pressure Res. https://doi.org/10.1080/08957959.2020.1863398

Su C, Liu YG, Wang ZG, Song W, Asimow PD, Tang HF, Xie HS (2017) Equation of state of liquid bismuth and its melting curve from ultrasonic investigation at high pressure. Phys B 524:154–162

Wang ZG, Liu YG, Zhou WG, Song W, Bi Y, Lie L, Xie HS (2013) Sound velocity in water and ice up to 4.2 GPa and 500 K on multi-anvil apparatus. Chin Phys Lett 30:054302

Wang XB, Chen T, Qi XT, Zou YT, Kung J, Yu T, Wang YB, Liebermann RC, Li BS (2015) Acoustic travel time gauges for in-situ determination of pressure and temperature in multi-anvil apparatus. J Appl Phys 118:065901

Xie HS (1997) Introduction to the Earth's Interior Materials Science. Science Press, Beijing **(in Chinese)**

Xie HS, Zhang YM, Xu HG, Hou W, Guo J (1993) A new method of measurement for elastic wave velocities in minerals and rocks at high temperature and high pressure and its significance. Sci China (Series B) 36:1276–1280

Xie HS, Zhou WG, Zhao ZD, Li YW, Guo J, Xu ZM, Xu JA (1998) Measurement of elastic wave velocities in rocks at high temperature and high pressure. Earth Sci Front 5:329–337 **(in Chinese)**

Xie HS, Zhou WG, Liu YG, Guo J, Hou W, Zhao ZD (2002) Comparative experimental study on several methods for measuring elastic wave velocities in rocks at high pressure. Sci China (Series D) 45:990–998

Xu L, Bi Y, Li XH, Wang Y, Cao XX, Cai LC, Wang ZG, Meng CM (2014) Phase diagram of tin determined by sound velocity measurements on multi-anvil apparatus up to 5 GPa and 800 K. J Appl Phys 115:164903

Xu M, Jing ZC, Chantel J, Jiang PX, Yu T, Wang YB (2018) Ultrasonic velocity of diopside liquid at high pressure and temperature: constraints on velocityreduction in the upper mantle due topartial melts. J Geophys Res Solid Earth 123:8676–8690

Yoneda A (1990) Pressure derivatives of elastic constants of single crystal MgO and $MgAl_2O_4$. J Phys Earth 38:19–55

Zhou WG, Fan DW, Liu YG, Xie HS (2011) Measurements of wave velocity and electrical conductivity of an amphibolite from southwestern margin of the Tarim Basin at pressures to 1.0 GPa and temperatures to 700 °C:comparison with field observations. Geophys J Int 187:1393–1404

Zhou CY, Jin ZM, Wang YB, Wang C, Zhang YF (2016) Sound velocity measurement of minerals and rocks at mantle transition zone conditions using ultrasonic and multianvil techniques. Earth Sci 41:1451–1460 **(in Chinese)**